

# Pressure drop, flow pattern and hold-up measurements of gas–liquid flow in pipes

S. Vestøl, A. S. Kumara & M. C. Melaaen  
*Telemark University College, Norway*

## Abstract

This paper presents detailed measurements on gas–liquid flows in horizontal and slightly inclined pipes. The mixture velocities, liquid fractions and pipe inclinations used in the experiments are in a range that is commonly used in transportation of unprocessed gas in offshore oil and gas industry. The experimental activities were performed using the multiphase flow loop at Telemark University College, Porsgrunn, Norway. The experiments were conducted in a 15 m long, 56 mm diameter, inclinable steel pipe using Exxsol D60 oil (density 793 kg/m<sup>3</sup> and viscosity 1.3 mPa·s), water (density 999 kg/m<sup>3</sup> and viscosity 0.89 mPa·s) and air (density 1.22 kg/m<sup>3</sup> and viscosity 0.018 mPa·s) as test fluids. Mixture velocities of 5, 10 and 15 m/s, liquid fractions of 0.0010, 0.0025, 0.0050, 0.0075 and 0.0100 and pipe inclinations of -5°, -1°, 0, +1° and +5° from horizontal were investigated. The time-averaged cross-sectional distributions of gas and liquid phases were measured using a single-beam gamma densitometer. The characterization of flow patterns and identification of their boundaries were performed using high-speed videos, still pictures and live observations. Seven different flow patterns were identified for gas liquid flow in horizontal and slightly inclined pipes. The pressure drop and liquid hold-up measurements were also reported.

*Keywords:* gas–liquid flow, mixture velocity, hold-up, pressure drop, horizontal flow, inclined flow, liquid fraction, flow pattern, gamma densitometer.

## 1 Introduction

The demand for natural gas is increasing worldwide, and production of natural gas is becoming a more and more important part of the petroleum industry. To produce natural gas from offshore reservoirs, the unprocessed gas has to be



transported from the wells to processing equipment. With increased knowledge about multiphase flow, subsea fields where the unprocessed gas is transported over long distances have become technically possible. This can dramatically reduce the cost of petroleum production and make marginal fields profitable that would otherwise not be economically viable. The transportation distance can be over 100 km long for some oil and gas fields in the Norwegian Continental Shelf.

Transportation of unprocessed natural gas presents many challenges including challenges related to multiphase flow phenomena. Due to condensation as the temperature decrease through the transport pipelines, multiphase flow will appear also from wells that at reservoir conditions produce only gas. Under such circumstances gas–liquid flow with low liquid fraction is of common occurrence. To design and operate gas pipelines it is important to understand how the liquid affects the flow. Liquid hold-up and pressure drop are two of the three important characteristics of gas–liquid flow, the other being the flow pattern. The availability of detailed measurements of these characteristics is of great value when studying gas–liquid flow phenomena in oil and gas industry.

## 2 Experimental set-up

The experiments were performed using the multiphase flow facility at Telemark University College (TUC), Porsgrunn, Norway.

### 2.1 Multiphase flow facility

The multiphase flow facility at TUC has been presented by Kumara *et al.* [1] and Sondre [2]. Three phases are available in the multiphase flow facility: gas, oil and water. Oil and water are stored in separate tanks (T100 and T101). Seven different pumps (P100, P101, P102, P103, P104, P105 and P106) are available to circulate the liquid phases through the system. The gas is taken from the central pressurized air system in the building, and the gas flow rate is controlled with a pneumatic control valve (V131). The three phases are mixed at the inlet of the test section (M100) designed to initiate separated flow. The test section is made of steel, except for two short plastic sections. A 0.8 m long transparent acrylic section is used to allow visual observations of the flow and a 0.4 m long polypropylene section is used to allow measurements with the gamma densitometer. The inner diameter of the steel pipe is 56.3 mm. A gas–liquid separator (R120) is located immediately downstream the test section. The liquid outlet of the gas–liquid separator is connected to an oil–water separator (R100) located at a lower elevation where the oil and water phases are separated and returned to their respective storage tanks (T100 and T101). Table 1 lists some important properties for the available fluids under atmospheric conditions.

There are three pressure transmitters connected to the test section. PDT120 measures the pressure drop over a distance of 10.21 m from the inlet of the test section. This measurement includes inlet effects. PDT121 measures the pressure drop over the last part of the test section, and here without the effects closest to



the inlet. The distance of this pressure drop measurement is 5.37 m ending at the same place as the PDT120 measurements. The inlet gauge pressure is measured with PT131.

There are six Coriolis flow meters installed, one for low flow rates and one for high flow rates for each phase. The accuracy of the density measurements are  $\pm 1 \text{ kg/m}^3$  for FT109B and FT114B, and  $\pm 0.5 \text{ kg/m}^3$  for FT110, FT115, FT131 and FT132. The temperature measurement accuracy is  $\pm 1^\circ\text{C}$ ,  $\pm 0.5\%$  of reading in  $^\circ\text{C}$ . In addition, liquid flow rates are also measured using two turbine flow meters (FT109A and FT114A) installed in the flow facility.

A controller based on LabView<sup>®</sup> is used for setting gas and liquid inflow rates and selecting appropriate pumps and flow meters. The flow rates are controlled by an automatic control loop which uses the flow meter readings to adjust the pump speeds and valve openings. The flow rate from P100, P101, P102, P103 and P104 are controlled by adjusting the pump speeds, while P105, P106 and the gas flow rate are controlled by adjusting control valve V131, V168 and V177 respectively.

Table 1: Fluid properties.

	Gas	Oil	Water
Fluid	Air	Exxsol D60	Tap water
Density at $15^\circ\text{C}$	$1.22 \text{ kg/m}^3$	$793 \text{ kg/m}^3$	$999 \text{ kg/m}^3$
Viscosity at $25^\circ\text{C}$	$0.018 \text{ mPa}\cdot\text{s}$	$1.3 \text{ mPa}\cdot\text{s}$	$0.89 \text{ mPa}\cdot\text{s}$
Surface tension at $25^\circ\text{C}$		$25.9 \text{ mN/m}$	$72.0 \text{ mN/m}$

## 2.2 Investigated flow conditions

The mixture velocity,  $U_m$ , is defined as follows:

$$U_m = \frac{Q_a + Q_l}{A} \quad (1)$$

where  $Q_a$  and  $Q_l$  are the inlet volumetric flow rates of air and liquid, respectively and  $A$  is the pipe cross-sectional area. In the present work, mixture velocities of 5, 10 and 15 m/s were studied. The inlet liquid fraction,  $\lambda_l$ , is defined as:

$$\lambda_l = \frac{Q_l}{Q_a + Q_l} \quad (2)$$

The experiments were performed at inlet liquid fractions of 0.0010, 0.0025, 0.0050, 0.0075 and 0.0100 and at pipe inclinations of  $-5^\circ$ ,  $-1^\circ$ ,  $0^\circ$ ,  $+1^\circ$  and  $+5^\circ$  from horizontal. All the experiments are performed for air–water and air–oil flows.

### 3 Results and discussion

The flow patterns were determined based on high-speed videos, still pictures and live observations taken during the experiments.

Only two main flow patterns appear in the experiments: stratified flow and slug flow. Several types of stratified flows are observed and have been categorized into 6 sub flow patterns, so a total of 7 flow patterns have been observed. The characteristics of those 7 flow patterns are described below. The observed flow patterns show a good agreement with the flow pattern maps presented by Taitel and Dukler [3] and Barnea *et al.* [4].

#### 3.1 Stratified smooth flow (ss)

In stratified smooth flow the gas and liquid is totally separated. The liquid flows in a layer at the bottom of the pipe, and the gas flows above. There are no interfacial waves and no entrainment. This flow pattern is observed for air–oil flows with low mixture velocity and low liquid fraction at horizontal and downward pipe inclinations. Pictures of a typical stratified smooth flow are given in Figure 1 for horizontal air–water flow with mixture velocity 5 m/s and liquid fraction 0.0010.

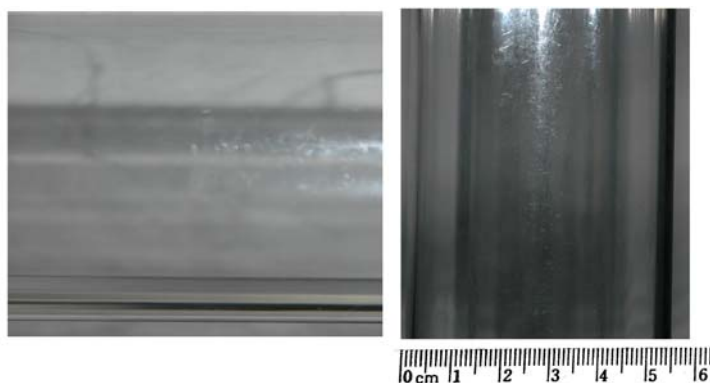


Figure 1: Pictures of a typical stratified smooth flow. Seen from the side (left) and from above (right).

#### 3.2 Stratified wavy flow without entrainment (s)

In stratified wavy flow without entrainment the gas and liquid phases are separated with liquid flowing at the bottom of the pipe and gas flowing above. Waves are present at the interface, but there is no entrainment. This flow pattern is observed for air–water flows with low mixture velocity and low liquid fractions. It is also observed for air–oil flows with low mixture velocity and high liquid fractions. Figure 2 gives pictures of a typical stratified wavy flow without entrainment. This is from a horizontal air–water flow with mixture velocity 5 m/s and liquid fraction 0.0100.

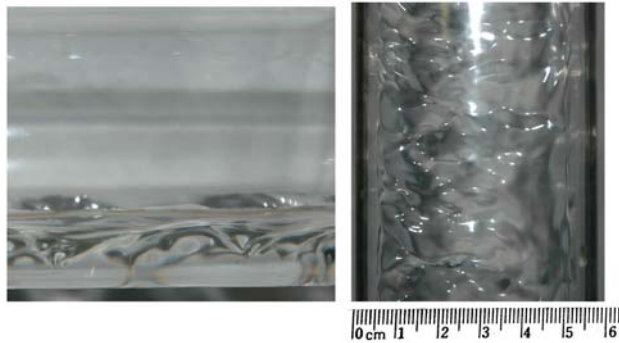


Figure 2: Pictures of a typical stratified wavy flow without entrainment. Seen from the side (left) and from above (right).

### 3.3 Stratified wavy flow with gas bubbles in liquid phase (sb)

Stratified wavy flow with gas bubbles in the liquid phase is very similar to the stratified wavy flow without entrainment flow pattern described above. The difference is that gas bubbles are entrained in the liquid layer in the stratified wavy flow. This flow pattern appears in horizontal and downwardly inclined air–oil flows with mixture velocity 10 m/s and liquid fraction 0.0010. Pictures of one example are given in Figure 3. This is from an air–oil flow with mixture velocity 10 m/s, liquid fraction 0.0010 and  $-5^\circ$  pipe inclination.

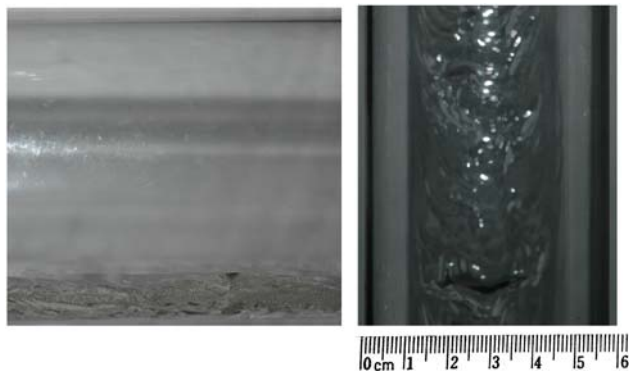


Figure 3: Pictures of a typical stratified wavy flow with gas bubbles in liquid phase. Seen from the side (left) and from above (right).

### 3.4 Stratified wavy flow with liquid droplets in gas phase (sd)

In stratified wavy flow with liquid entrainment in the gas phase there are large waves at the interface between the liquid layer at the bottom and the gas layer above. Liquid droplets are released from the wavy interface and dispersed into the gas phase. This flow pattern appears for air–water flows with high mixture

velocity. Pictures of this flow pattern are given in Figure 4. This is from a horizontal air–water flow with mixture velocity 10 m/s and inlet liquid fraction 0.0100.

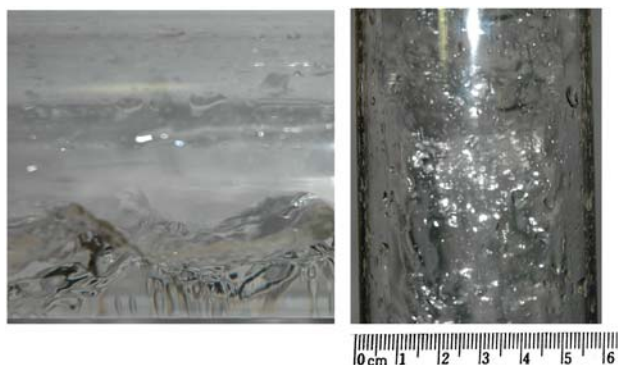


Figure 4: Pictures of a typical stratified wavy flow with liquid droplets in gas phase. Seen from the side (left) and from above (right).

### 3.5 Stratified wavy flow with gas bubbles in liquid phase and liquid droplets in gas phase (sbd)

Stratified wavy flow with gas bubbles in the liquid phase and liquid droplets in the gas phase is similar to the stratified wavy flow with liquid droplets in the gas phase flow pattern, but here gas bubbles are entrained in the liquid layer in addition to the liquid droplets entrained in the gas phase. This flow pattern appears in air–oil flows with high mixture velocity. Pictures are given in Figure 5. This shows a horizontal air–oil flow with mixture velocity 10 m/s and liquid fraction 0.0100.

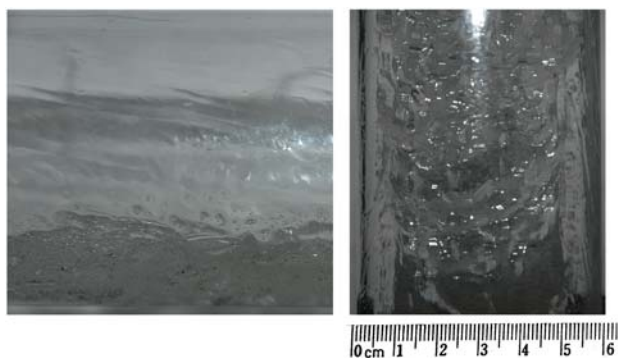


Figure 5: Pictures of a typical stratified wavy flow with gas bubbles in liquid phase and liquid droplets in gas phase. Seen from the side (left) and from above (right).

### 3.6 Transition flow pattern (tr)

The transition flow appears in the experiments with high mixture velocity and high liquid fraction. It is mainly a stratified flow type where most of the liquid flows at the bottom of the pipe and the gas flows above it, but it also have elements from annular flow and slug flow. In this flow pattern the pipe wall is completely covered with a liquid film most of the time, like in annular flow, but sometimes parts of the wall dries up and is only covered by droplets. The interfacial waves are large, and some of the waves reach all the way up to the top of the pipe and starts to form slugs. Pictures of transition flow pattern are shown in Figure 6. The pictures are from a horizontal air–water flow with mixture velocity 15 m/s and liquid fraction 0.0100.

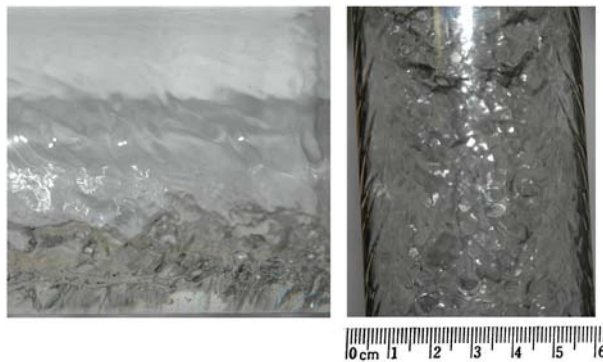


Figure 6: Pictures of a typical transition flow pattern. Seen from the side (left) and from above (right).

### 3.7 Slug flow (sl)

Slug flow is a transient flow pattern with alternating regions of stratified or annular flow and regions of dispersed flow following each other. This flow pattern appears in the experiments for low mixture velocities in upwardly inclined pipes. In the experiments the slugs are generated by the pipe inclination where gravity works to drag the flow backwards. Due to the high density of the liquid, gravity can become dominant for the liquid layer when the interfacial friction is low at low mixture velocities. This makes the liquid flow backwards, at least at the bottom of the liquid layer, which leads to liquid accumulation at the pipe inlet. Eventually the accumulated liquids blocks the entire pipe cross-section and gas is accumulating behind the liquid plug until the pressure build-up is enough to push out the blocking liquid. When that happens the liquid flows through the pipe as a slug at high velocity. When the slug has left the system, the velocities decrease again and after some time the backwards flow of liquid reappears and the slug cycle repeats. Figure 7 shows pictures of different phases of the slug cycle. The pictures are taken from an air–water flow with mixture velocity 5 m/s, liquid fraction 0.0050 and pipe inclination  $+5^\circ$ .

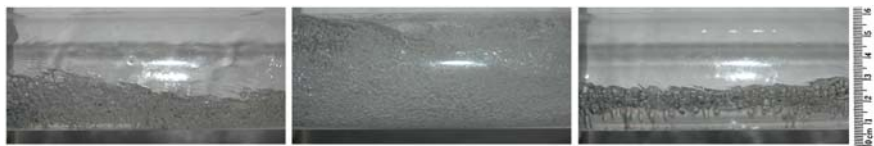


Figure 7: Pictures of different phases in slug flow. Slug bubble just before the slug front seen from the side (left), slug body seen from the side (middle), slug bubble just after the slug has passed seen from the side (right).

3.8 Flow pattern maps for air–water and air–oil flows

The flow pattern determination is based on visual observations and is subject to subjective judgments. The observed flow patterns of air–water and air–oil flows are presented in Table 2 and Table 3, respectively.

Table 2: Flow patterns for air–water flows,  $\beta$  = pipe inclination from horizontal.

	$U_m = 5 \text{ m/s}$	$U_m = 10 \text{ m/s}$	$U_m = 15 \text{ m/s}$
$\beta = -5^\circ$	$\lambda_L = 0.0010: \text{s}$ $\lambda_L = 0.0025: \text{s}$ $\lambda_L = 0.0050: \text{s}$ $\lambda_L = 0.0075: \text{s}$ $\lambda_L = 0.0100: \text{s}$	$\lambda_L = 0.0010: \text{s}$ $\lambda_L = 0.0025: \text{s}$ $\lambda_L = 0.0050: \text{s}$ $\lambda_L = 0.0075: \text{s}$ $\lambda_L = 0.0100: \text{sd}$	$\lambda_L = 0.0010: \text{sd}$ $\lambda_L = 0.0025: \text{sd}$ $\lambda_L = 0.0050: \text{sd}$ $\lambda_L = 0.0075: \text{sd}$ $\lambda_L = 0.0100: \text{sd}$
$\beta = -1^\circ$	$\lambda_L = 0.0010: \text{s}$ $\lambda_L = 0.0025: \text{s}$ $\lambda_L = 0.0050: \text{s}$ $\lambda_L = 0.0075: \text{s}$ $\lambda_L = 0.0100: \text{s}$	$\lambda_L = 0.0010: \text{s}$ $\lambda_L = 0.0025: \text{s}$ $\lambda_L = 0.0050: \text{s}$ $\lambda_L = 0.0075: \text{sd}$ $\lambda_L = 0.0100: \text{sd}$	$\lambda_L = 0.0010: \text{sd}$ $\lambda_L = 0.0025: \text{sd}$ $\lambda_L = 0.0050: \text{sd}$ $\lambda_L = 0.0075: \text{sd}$ $\lambda_L = 0.0100: \text{tr}$
$\beta = 0^\circ$	$\lambda_L = 0.0010: \text{s}$ $\lambda_L = 0.0025: \text{s}$ $\lambda_L = 0.0050: \text{s}$ $\lambda_L = 0.0075: \text{s}$ $\lambda_L = 0.0100: \text{s}$	$\lambda_L = 0.0010: \text{s}$ $\lambda_L = 0.0025: \text{s}$ $\lambda_L = 0.0050: \text{sd}$ $\lambda_L = 0.0075: \text{sd}$ $\lambda_L = 0.0100: \text{sd}$	$\lambda_L = 0.0010: \text{sd}$ $\lambda_L = 0.0025: \text{sd}$ $\lambda_L = 0.0050: \text{sd}$ $\lambda_L = 0.0075: \text{tr}$ $\lambda_L = 0.0100: \text{tr}$
$\beta = +1^\circ$	$\lambda_L = 0.0010: \text{sl}$ $\lambda_L = 0.0025: \text{sl}$ $\lambda_L = 0.0050: \text{sl}$ $\lambda_L = 0.0075: \text{sl}$ $\lambda_L = 0.0100: \text{sl}$	$\lambda_L = 0.0010: \text{s}$ $\lambda_L = 0.0025: \text{s}$ $\lambda_L = 0.0050: \text{sd}$ $\lambda_L = 0.0075: \text{sd}$ $\lambda_L = 0.0100: \text{sd}$	$\lambda_L = 0.0010: \text{sd}$ $\lambda_L = 0.0025: \text{sd}$ $\lambda_L = 0.0050: \text{sd}$ $\lambda_L = 0.0075: \text{tr}$ $\lambda_L = 0.0100: \text{tr}$
$\beta = +5^\circ$	$\lambda_L = 0.0010: \text{sl}$ $\lambda_L = 0.0025: \text{sl}$ $\lambda_L = 0.0050: \text{sl}$ $\lambda_L = 0.0075: \text{sl}$ $\lambda_L = 0.0100: \text{sl}$	$\lambda_L = 0.0010: \text{sl}$ $\lambda_L = 0.0025: \text{sl}$ $\lambda_L = 0.0050: \text{sl}$ $\lambda_L = 0.0075: \text{sl}$ $\lambda_L = 0.0100: \text{sl}$	$\lambda_L = 0.0010: \text{sd}$ $\lambda_L = 0.0025: \text{sd}$ $\lambda_L = 0.0050: \text{tr}$ $\lambda_L = 0.0075: \text{tr}$ $\lambda_L = 0.0100: \text{tr}$





Table 3: Flow patterns for air–oil flows,  $\beta$  = pipe inclination from horizontal.

	$U_m = 5 \text{ m/s}$	$U_m = 10 \text{ m/s}$	$U_m = 15 \text{ m/s}$
$\beta = -5^\circ$	$\lambda_L = 0.0010$ : ss $\lambda_L = 0.0025$ : ss $\lambda_L = 0.0050$ : s $\lambda_L = 0.0075$ : s $\lambda_L = 0.0100$ : s	$\lambda_L = 0.0010$ : sb $\lambda_L = 0.0025$ : sbd $\lambda_L = 0.0050$ : sbd $\lambda_L = 0.0075$ : sbd $\lambda_L = 0.0100$ : sbd	$\lambda_L = 0.0010$ : sbd $\lambda_L = 0.0025$ : sbd $\lambda_L = 0.0050$ : sbd $\lambda_L = 0.0075$ : sbd $\lambda_L = 0.0100$ : sbd
$\beta = -1^\circ$	$\lambda_L = 0.0010$ : ss $\lambda_L = 0.0025$ : ss $\lambda_L = 0.0050$ : s $\lambda_L = 0.0075$ : s $\lambda_L = 0.0100$ : s	$\lambda_L = 0.0010$ : sb $\lambda_L = 0.0025$ : sbd $\lambda_L = 0.0050$ : sbd $\lambda_L = 0.0075$ : sbd $\lambda_L = 0.0100$ : sbd	$\lambda_L = 0.0010$ : sbd $\lambda_L = 0.0025$ : sbd $\lambda_L = 0.0050$ : sbd $\lambda_L = 0.0075$ : sbd $\lambda_L = 0.0100$ : sbd
$\beta = 0^\circ$	$\lambda_L = 0.0010$ : ss $\lambda_L = 0.0025$ : ss $\lambda_L = 0.0050$ : s $\lambda_L = 0.0075$ : s $\lambda_L = 0.0100$ : s	$\lambda_L = 0.0010$ : sb $\lambda_L = 0.0025$ : sbd $\lambda_L = 0.0050$ : sbd $\lambda_L = 0.0075$ : sbd $\lambda_L = 0.0100$ : sbd	$\lambda_L = 0.0010$ : sbd $\lambda_L = 0.0025$ : sbd $\lambda_L = 0.0050$ : sbd $\lambda_L = 0.0075$ : sbd $\lambda_L = 0.0100$ : tr
$\beta = +1^\circ$	$\lambda_L = 0.0010$ : sl $\lambda_L = 0.0025$ : sl $\lambda_L = 0.0050$ : sl $\lambda_L = 0.0075$ : sl $\lambda_L = 0.0100$ : sl	$\lambda_L = 0.0010$ : sbd $\lambda_L = 0.0025$ : sbd $\lambda_L = 0.0050$ : sbd $\lambda_L = 0.0075$ : sbd $\lambda_L = 0.0100$ : sbd	$\lambda_L = 0.0010$ : sbd $\lambda_L = 0.0025$ : sbd $\lambda_L = 0.0050$ : sbd $\lambda_L = 0.0075$ : tr $\lambda_L = 0.0100$ : tr
$\beta = +5^\circ$	$\lambda_L = 0.0010$ : sl $\lambda_L = 0.0025$ : sl $\lambda_L = 0.0050$ : sl $\lambda_L = 0.0075$ : sl $\lambda_L = 0.0100$ : sl	$\lambda_L = 0.0010$ : sl $\lambda_L = 0.0025$ : sl $\lambda_L = 0.0050$ : sl $\lambda_L = 0.0075$ : sl $\lambda_L = 0.0100$ : sl	$\lambda_L = 0.0010$ : sbd $\lambda_L = 0.0025$ : sbd $\lambda_L = 0.0050$ : tr $\lambda_L = 0.0075$ : tr $\lambda_L = 0.0100$ : tr

It is observed that the horizontal and downwardly inclined conditions give stratified flow. Upwardly inclined conditions give slug flow for low mixture velocities, and stratified flow for high mixture velocities. For horizontal and upwardly inclined conditions with high liquid fraction and the highest mixture velocity, the transition flow pattern appears.

Stratified flow with entrainment appears for high liquid fractions and high mixture velocities. Entrainment appears more easily for the air–oil flows than for the air–water flows. For air–oil flow only mixture velocity 5 m/s gives stratified flow without entrainment, while stratified flow without entrainment is observed also for mixture velocity 10 m/s for the air–water cases with the lowest liquid fractions. The decreased entrainment in the air–water flows compared to the air–oil flows is probably caused by the high surface tension of water. With higher surface tension, more force is needed to break off droplets from the liquid layer.

Entrained bubbles in the liquid phase are always present in the air–oil cases where liquid droplets are entrained in the gas phase. Entrained bubbles in the

liquid phase also appear for a few of the air–oil cases where no liquid droplets are observed in the gas phase. This happens for horizontal and downwardly inclined air–oil flows with mixture velocity 10 m/s and liquid fraction 0.0010. Entrained bubbles in the liquid phase never appear for the air–water cases. This is probably because the surface tension of water is too high to allow air bubbles to enter the liquid phase with the studied flow conditions.

Stratified smooth flow only appears for horizontal and downwardly inclined oil–water flows with low liquid fraction and the lowest mixture velocity. Stratified smooth flow does not appear for any of the air–water flows, probably because the viscosity of water is lower than for oil.

### 3.9 Pressure drop and liquid hold-up measurements

There are three pressure transmitters in the experimental set-up, PDT120, PDT121 and PT131. Pressure drop measurements from PDT121 are reported as it does not include inlet effects. PDT121 measures the pressure drop over a distance of 5.37 m towards the end of the test section.

The liquid hold-up for gas–liquid flow can be defined as:

$$\text{Liquid hold-up} = \frac{A_l}{A} \quad (3)$$

where  $A_l$  is the cross-sectional area occupied by liquid phase, i.e., oil or water. The vertical distance from the bottom of the pipe to the point, where the local liquid volume fraction is equal to 0.50 is considered as the interface height and the interface is treated as a flat surface in order to estimate the flow areas for different phases. It is possible to measure the liquid fractions as a function of time at a given cross-section of the pipe, so called in-situ liquid hold-up. In gas–liquid flow, the in-situ liquid hold-up is time dependent due to interfacial waves, interface mixing and slug flow. The hold-up values reported in this paper are estimated by using the time average local phase fraction measurements from gamma densitometer.

The measured pressure drop and hold-up data of air–water and air–oil flows at different pipe inclinations are presented in Figures 8–12. The measured hold-up values of air–water and air–oil flow at similar mixture velocities and pipe inclinations show small variations. The most noticeable difference is in the upward and downward flow results. The flow pattern changes from an intermittent flow regime (transition and slug flow) in upward flow to stratified flow regime in downward flow. In case of downward flow the liquid moves faster due to the gravity effect resulting in lower liquid hold-ups while in upward flow this effect is reversed and the liquid moves slower resulting in intermittent flow and higher hold-ups. As shown in Figure 9(b), in downward stratified flow at pipe inclination  $-1^\circ$ , the liquid hold-up becomes independent of mixture velocity over a wide range of the gas flow rate and is a function of liquid flow rate. This shows a good agreement with the results presented by Kokal and Stanislav [5]. However, the liquid hold-up increases as mixture velocity increases for downwardly inclined flow at pipe inclination  $-5^\circ$ . This may due to

the interfacial waves and complex interfacial mixing phenomena observed at this pipe inclination. The inclination angle has a little effect on the liquid hold-up in upwardly inclined flow. In general, the hold-up increases slightly for the higher inclination angles. For horizontal and upwardly inclined flows, higher hold-up values are observed at lower mixture velocities as expected. However, lower hold-up values are recorded at lower mixture velocities for downwardly inclined flow at pipe inclination  $-5^\circ$ . In general, the measured hold-up data shows a good comparison with the results presented by Kokal and Stanislav [5], Andritsos and Hanratty [6]). It must be noted that the experimental procedure for measuring hold-up will give slightly biased results for transient flows, like slug flow in upwardly inclined pipes. The liquid hold-ups have been measured based on the averaged gamma densitometer results over a time period covering a number of slugs. During this time period there are long periods with low hold-up followed by short periods with high hold-up when slugs pass through the gamma densitometer. The relation between gamma counts/second and hold-up is not completely linear. As a result, the time averaging of the gamma measurements will give slightly lower hold-up measurements for slug flows in upwardly inclined pipes.

The pressure drop increases with the inlet liquid flow rate and mixture velocity. As shown in Figure 10(a), slightly higher pressure drops are measured for air–water flow compared to air–water flow at low mixture velocity of 5 m/s. This may be attributed to the increased viscous effects of air–oil flow at lower mixture velocity. This effect was not observed for other pipe inclinations at mixture velocity 5 m/s. At higher mixture velocities, similar pressure drops are observed for both air–oil and air–water flows. The pressure drops at mixture velocity of 5 m/s for horizontal and downwardly inclined flows are relatively unaffected by the inlet liquid flow rates. In general, pressure drop decreases as the pipe is downwardly inclined due to gravitational acceleration. On the other hand, upwardly inclined flows are predominantly intermittent, which is associated with higher pressure drops. As a result, higher pressure drops are observed in upwardly inclined flows where slug and transition flow patterns are observed.

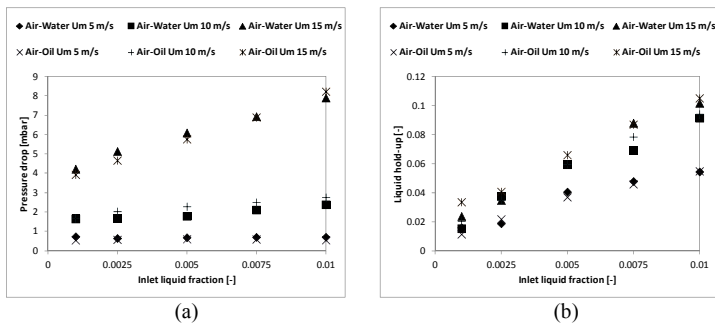


Figure 8: Pressure drop and hold-up measurements for air–water and air–oil flows at pipe inclination  $-5^\circ$ . (a) Pressure drop, (b) Hold-up.

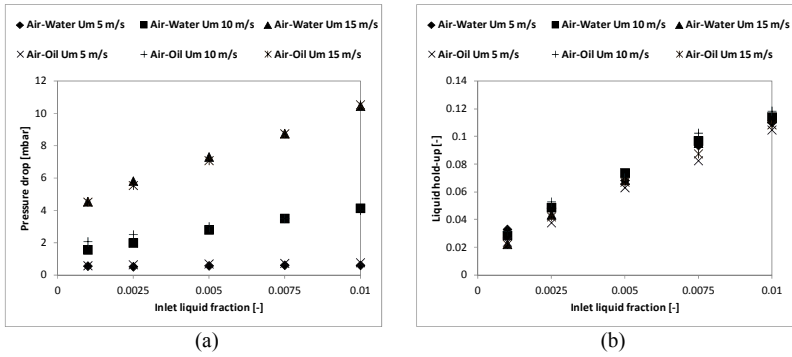


Figure 9: Pressure drop and hold-up measurements for air–water and air–oil flows at pipe inclination  $-1^\circ$ . (a) Pressure drop, (b) Hold-up.

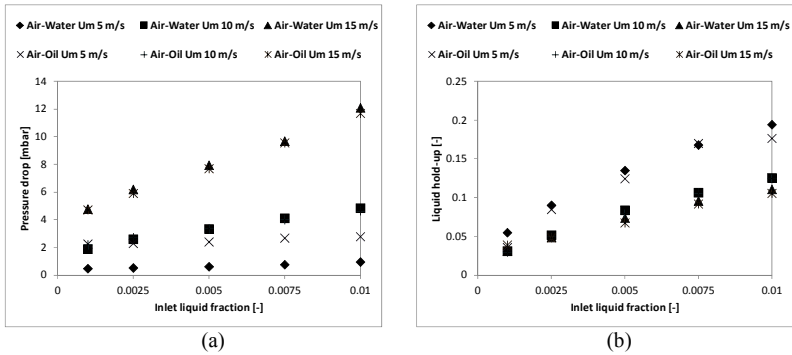


Figure 10: Pressure drop and hold-up measurements for air–water and air–oil flows at pipe inclination  $0^\circ$ . (a) Pressure drop, (b) Hold-up.

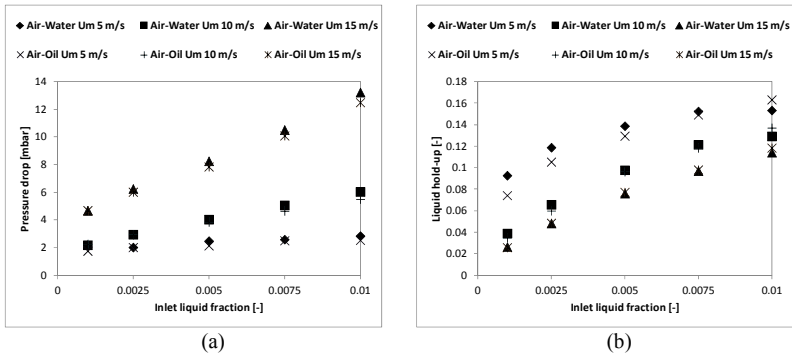


Figure 11: Pressure drop and hold-up measurements for air–water and air–oil flows at pipe inclination  $+1^\circ$ . (a) Pressure drop, (b) Hold-up.

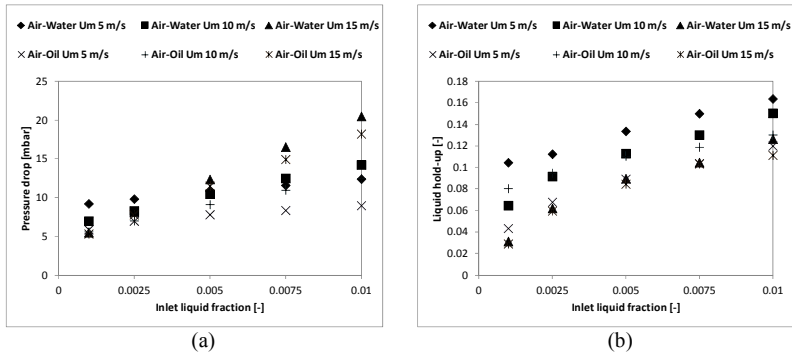


Figure 12: Pressure drop and hold-up measurements for air–water and air–oil flows at pipe inclination +5°. (a) Pressure drop, (b) Hold-up.

## 4 Conclusions

The flow patterns, pressure drop and liquid hold-up measurements are presented for air–water and air–oil flows with mixture velocities in the range 5 m/s to 15 m/s, inlet liquid fractions in the range 0.0010 to 0.0100 and pipe inclinations in the range -5° to +5°.

The flow patterns were determined based on high-speed videos, still pictures and live observations taken during the experiments. Only two main flow patterns appear in the experiments: Stratified flow and slug flow. Several types of stratified flow were observed and have been categorized into 6 sub flow patterns, so a total of 7 flow patterns have been observed.

Both liquid hold-up and pressure drop were affected by the inclination angle. Stratified flow was found to be associated with low liquid hold-ups and pressure drops. Upwardly intermittent flow was associated with high liquid hold-ups and pressure drops.

## References

- [1] Kumara, W.A.S. Halvorsen, B.M. & Melaaen, M.C., Particle image velocimetry for characterizing the flow structure of oil–water flow in horizontal and slightly inclined pipes, *Chemical Engineering Science*, **65**, pp. 4332–4349, 2010.
- [2] Sondre, V., Detailed measurements of gas/liquid flow with low liquid fractions and near horizontal pipes, PhD thesis, Telemark University College, 30<sup>th</sup> October 2013.
- [3] Taitel, Y. & Dukler, A.E., A model for predicting flow regime transition in horizontal and near horizontal gas–liquid flow, *AIChE J.* **22**, pp. 47–55, 1976.



- [4] Barnea, D., Shoham, O., Taitel, Y. & Dukler, A.E., Flow pattern transition for gas–liquid flow in horizontal and inclined pipes, *Int. J. Multiphase Flow*, **6**, pp. 217–225, 1980.
- [5] Kokal, S.L. & Stanislav, J.F., An experimental study of two-phase flow in slightly inclined pipes-II. Liquid hold-up and pressure drop, *Chemical Engineering Science*, **44(3)**, pp. 681–693, 1989.
- [6] Andritsos, N. & Hanratty, T.J., Influence on interfacial waves in stratified gas–liquid flows, *A.I.Ch.E.J.*, **33**, pp. 444–454, 1987.

